

Bimodal Evans–Polanyi Relationships in Dioxirane Oxidations of sp^3 C–H: Non-perfect Synchronization in Generation of Delocalized Radical Intermediates

Fengjiao Liu,^{†,‡} Zhongyue Yang,[‡] Yanmin Yu,^{‡,||} Ye Mei,^{*,†,§,||} and K. N. Houk^{*,‡,||}

[†]State Key Laboratory of Precision Spectroscopy, School of Physics and Materials Science, East China Normal University, Shanghai 200062, China

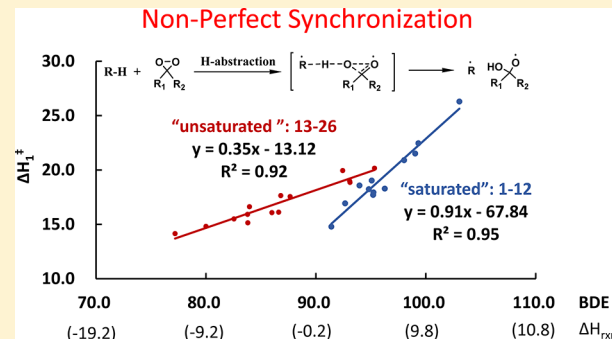
[‡]Department of Chemistry and Biochemistry, University of California, Los Angeles, California 90095, United States

[§]NYU-ECNU Center for Computational Chemistry at NYU Shanghai, Shanghai 200062, China

^{||}Beijing Key Laboratory for Green Catalysis and Separation, Department of Chemistry and Chemical Engineering, Beijing University of Technology, Beijing 100124, China

Supporting Information

ABSTRACT: The selectivities in C–H oxidations of a variety of compounds by DMDO have been explored with density functional theory. There is a linear Evans–Polanyi-type correlation for saturated substrates. Activation energies correlate with reaction energies or, equivalently, BDEs ($\Delta H_{\text{sat}}^{\ddagger} = 0.91 \cdot \text{BDE} - 67.8$). Unsaturated compounds, such as alkenes, aromatics, and carbonyls, exhibit a different correlation for allylic and benzylic C–H bonds ($\Delta H_{\text{unsat}}^{\ddagger} = 0.35 \cdot \text{BDE} - 13.1$). Bernasconi’s Principle of Non-Perfect Synchronization (NPS) is found to operate here. The origins of this phenomenon were analyzed by a Distortion/Interaction model. Computations indicate early transition states for H-abstractions from allylic and benzylic C–H bonds, but later transition states for the saturated. The reactivities are mainly modulated by the distortion energy and the degree of dissociation of the C–H bond. While the increase in barrier with higher BDE is not unexpected from the Evans–Polanyi relationship, two separate correlations, one for saturated compounds, and one for unsaturated leading to delocalized radicals, were unexpected.



INTRODUCTION

The selective functionalization of sp^3 C–H bonds is one of the current challenges in organic chemistry and is a powerful strategy for organic synthesis.^{1–6} Many reagents are now known for C–H functionalization, such as radicals, metal-oxo species, transition metals (Ru, Cr, Pd, etc.), and dioxiranes.^{7–9} Understanding how selectivity is controlled and predicted is one of the central challenges in this field. This work examines the reactivity–selectivity relationships for dioxirane oxidations of a variety of hydrocarbons and substituted hydrocarbons.

Dimethyldioxirane (DMDO) and methyl(trifluoromethyl)-dioxirane (TFDO) are outstanding reagents for selective oxidation of a variety of alkanes under mild conditions and without metal catalysts.^{10–14} Curci et al. pioneered in the use of dioxiranes for C–H oxidations, and they carried out a series of systematic investigations on mechanism.¹⁵ Dioxiranes can effect site-selective hydroxylations of target substrates and are used for “late-stage C–H oxidation”.^{16–19} Chen and Baran developed a two-phase strategy (“cyclase phase” and “oxidase phase”) to access oxidized terpenes.¹⁸ The approach combines the guided C–H functionalization with Curci’s TFDO oxidation. As exemplified in Figure 1a, a substrate with five

unactivated tertiary C–H bonds is only oxidized at the equatorial C–H bond.¹⁸ Figure 1b shows several other examples of selective C–H oxidations by dioxiranes.²⁰ Applications and site selectivity examples for C–H oxidation by dioxiranes are well documented.^{21–29}

Studies by Curci,¹⁵ Baran,^{20,30} Houk³¹ and others^{32,33} show that the observed selectivities may result from cooperation of reactivity factors that involve electronic, steric, and strain effects in transition states. Similar factors have also been reported by White in C–H oxidation reactions of complex molecules by a nonheme, iron-based system.^{34,35} In 1982, Tedder showed there is a correlation between rate constants and activation parameters with C–H bond strengths (Evans–Polanyi-type correlation, also known as Bell–Evans–Polanyi or Brønsted–Evans–Polanyi relationships) for H-abstraction by radicals.³⁶ Mayer et al. studied H-abstractions by CrO_2Cl_2 , MnO_4^- , and other coordination complexes³⁷ and pointed out that the Evans–Polanyi-type correlations should be universal. Furthermore, such correlations can be derived from fundamental

Received: July 28, 2017

Published: October 25, 2017

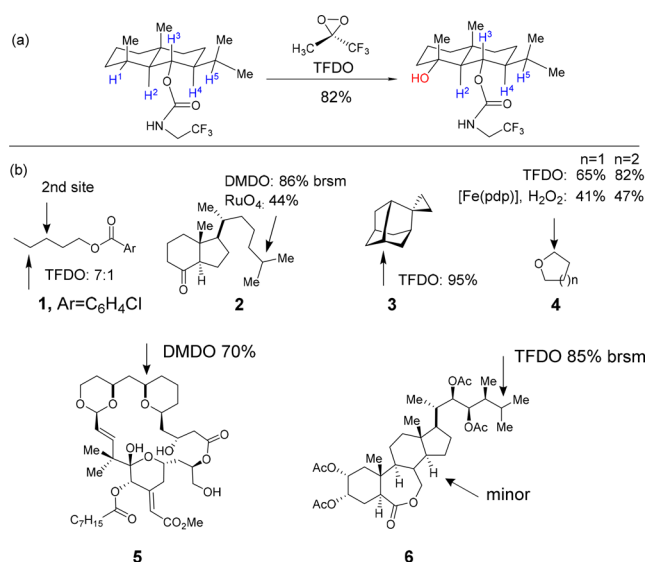


Figure 1. (a) Selectivities in “late-stage C–H oxidations” for the synthesis of terpenes by Baran.¹⁸ (b) Selective C–H oxidation examples from ref 20.

models of barrier formation according to Shaik et al.³⁸ We have explored the origins of selectivities in dioxirane reactions, considering especially the influence of bond dissociation energies (BDE), steric effects, and polar effects.

COMPUTATIONAL METHODS

Calculations were performed with Gaussian 09.³⁹ Energy minima and transition structures were optimized using UB3LYP with the 6-31G(d) basis set. Frequency analyses were carried out on these stationary points to verify if they correspond to energy minima or saddle points (transition states). Energies were recalculated at the UB3LYP/6-311++G(d,p) level for the optimized geometries. A keyword “stable = opt” was employed to obtain the unrestricted wave functions. The effectiveness of UB3LYP for geometry optimizations and energy calculations for this reaction has been demonstrated by numerous studies.^{31,40,41} Calculations with U ω B97X-D⁴² were also performed.

RESULTS AND DISCUSSION

For the hydroxylation of a C–H bond by DMDO, the H-abstraction-O-rebound mechanism (Figure 2) was shown to be most favorable with an open-shell singlet transition state in the rate-determining step (i.e., H-abstraction).^{14,31,40,41,43–47} H-abstraction results in a radical pair, and the rate of reaction is determined by the ease of H-abstraction by the dioxirane.

Previous studies have analyzed activation barriers on C–H abstractions with a variety of oxidizing reagents.^{37,38,48–51} For example, Shaik et al. demonstrated a linear correlation between the activation barrier and BDE for C–H oxidation by p450 CpdI,⁵¹ and Mayer et al. observed a linear correlation for the C–H oxidation by some metal–oxo complexes (CrO₂Cl₂, MnO₄[−]).³⁷ This indicates that radical stability, as quantified by BDE, is a determining factor for the activation barrier of C–H oxidation. In this work, a number of C–H bonds (Table 1) were studied to establish the structure–reactivity relationship in H-abstraction by DMDO, particularly, the relationship between reactivities and radical stabilities of substrates. The Distortion/Interaction model was employed to analyze the results,⁵² and divides the activation energy (ΔE^\ddagger) into the distortion energy (ΔE_d^\ddagger) and the energy of interaction ($\Delta E_{\text{inter}}^\ddagger$) between distorted fragments. The distortion energy is the energy

H-abstraction-O-rebound mechanism

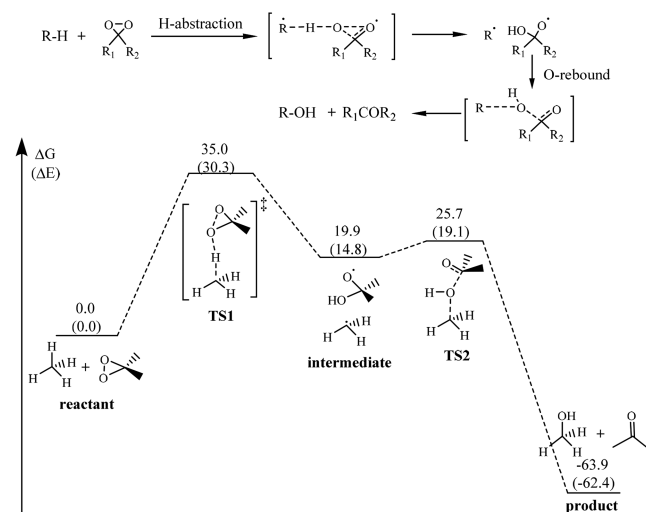


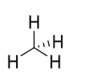
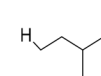
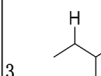
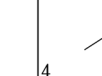
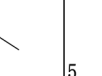
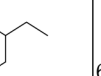
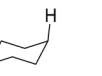
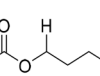
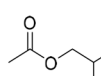
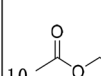
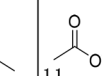
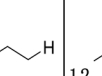
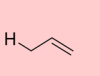
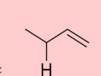
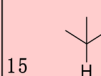

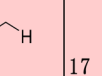
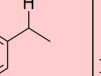
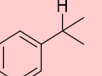
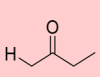
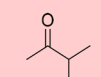
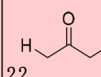
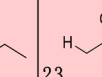
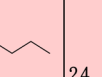
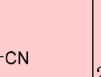
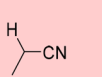
Figure 2. Free energy diagram of methane oxidation by DMDO in gas phase using UB3LYP/6-311++G(d,p)//UB3LYP/6-31G(d). All the energy terms are given in kcal/mol.

required to distort the substrates and the dioxirane into the geometries they have in the transition state without allowing interaction between the addends. Interaction energy is computed by the difference between the energy of the TS and the energies of two deformed fragments. The activation energy is then $\Delta E^\ddagger = \Delta E_d^\ddagger + \Delta E_{\text{inter}}^\ddagger$, where E is the electronic energy.

Various DFT methods were benchmarked against CASPT2 calculation (Table S1). UB3LYP best reproduces the reaction barrier by CASPT2, followed by the U ω B97X-D. On the other hand, B3LYP and ω B97X-D were benchmarked against experiment for compounds a–e oxidized by TFDO, as listed in the Table S2. In comparison, the experimental barriers are well reproduced by B3LYP, but systematically overestimated by ω B97X-D. The benzylic systems, d and e in Table S2, have experimental barriers that are even higher than those leading to the less stable secondary and nonplanar tertiary systems that certainly have higher BDEs. This indicates that the benzylic stabilization not fully manifested in the transition states for hydrogen abstraction. Consequently, we chose UB3LYP in our following studies, except otherwise mentioned. Table S3 summarizes the BDE, activation energy (ΔE_1^\ddagger), activation enthalpy (ΔH_1^\ddagger), activation free energy (ΔG_1^\ddagger), reaction enthalpy (ΔH_{rxn}), total distortion energy (ΔE_d^\ddagger), distortion energy of substrates ($\Delta E_d^\ddagger(\text{Alk})$), distortion energy of DMDO ($\Delta E_d^\ddagger(\text{DMDO})$), and interaction energy between distorted fragments ($\Delta E_{\text{inter}}^\ddagger$).

Reactivities versus Radical Stabilities or Reaction Energies. Radical stabilities are generally determined by BDEs. Figure 3 shows the relationship between the activation enthalpy and BDE (or ΔH_{rxn}) for the reactions of alkanes and substituted alkanes with DMDO. Figure 3a shows that overall there is only a rough correlation of activation barrier with BDE for all the calculated substrates, with $R^2 = 0.73$. The substrates were then classified into two categories, “saturated group” (substrates 1–12 in Table 1) and “unsaturated group” (substrates 13–26, containing the C–H directly adjacent to the $-\text{C}=\text{C}-$, $-\text{C}=\text{O}$, $-\text{CN}$, or benzene ring in Table 1). Figure 3b shows that both groups individually give good linear correlations between activation enthalpy and BDE, with R^2

Table 1. C–H Bonds for Which Oxidations Were Studied^a

1		2		3		4		5		6		7	
8		9		10		11		12					
13		14		15		16		17		18		19	
20		21		22		23		24		25		26	

^a1–12 are labeled as “saturated group”, and 13–26 are labeled as “unsaturated group” (containing the C–H directly adjacent to the –C=C–, –C=O, –CN, or benzene ring, leading to a conjugated radical).

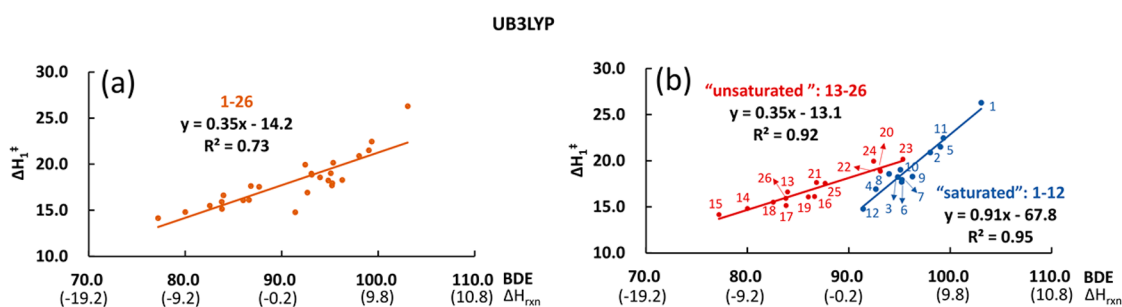


Figure 3. Activation enthalpy of H-abstraction (ΔH_1^\ddagger) versus C–H BDE (or ΔH_{rxn}). (a) Orange dots cover all substrates 1–26. (b) Red dots are C–H bonds in the “unsaturated group”. Blue dots are C–H bonds in the “saturated group”. Calculations are based on UB3LYP/6-311++G(d,p)//UB3LYP/6-31G(d). Energies are given in kcal/mol.

equal to 0.95 and 0.92, respectively. The activation enthalpies and BDEs were also plotted based on the calculations by the unrestricted ω B97X-D method, and correlations are shown in Figure 4a and Figure 4b. A similar tendency was found, with a poor linear correlation for all substrates ($R^2 = 0.76$), and a good correlation with the “saturated group” ($R^2 = 0.95$), but less so with the “unsaturated group” ($R^2 = 0.75$). Both calculations indicate that C–H oxidation of sp^3 C–H involves a bimodal correlation for “saturated” and “unsaturated” groups. The following analysis is based on the calculations by UB3LYP.

For the “saturated group”, the slope (0.91) is close to 1.0, indicating that the influence of substituents on the reaction barrier is almost as much as that on the radical stability. On the other hand, for the “unsaturated group”, the slope (0.35) is less than 0.5, radical stability has a relatively small effect on the barrier. The results are quite different from expectations based on the Hammond postulate⁵³ or from Marcus theory.^{54–56} In Brønsted or Evans–Polanyi relationships the slope is often about 0.5,⁵⁷ and in Marcus theory, which utilizes overlapping harmonic potential functions to describe reactant and product deformations along an electron-transfer coordinate, the slope for moderately exergonic or endergonic reactions is 0.5.⁵⁶ The harmonic oscillator model is particularly useful for high vibrational energies. However, for chemical bond dissociation, the harmonic potential is not an accurate representation of energies for extensive bond stretching. The C–H oxidations of the “saturated group” generally involve a later transition state than those of the “unsaturated group”, making the transition

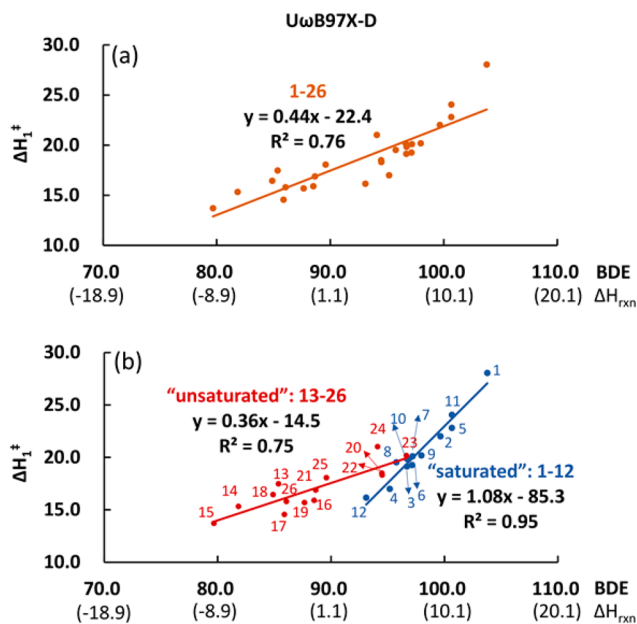


Figure 4. Activation enthalpy of H-abstraction (ΔH_1^\ddagger) versus C–H BDE (or ΔH_{rxn}). (a) Orange dots cover all substrates 1–26. (b) Red dots C–H bonds in the “unsaturated group”, blue dots are C–H bonds in the “saturated group”. Calculations are based U ω B97X-D/6-311++G(d,p)//U ω B97X-D/6-31G(d). Energies are given in kcal/mol.

state resemble the diradical intermediate both geometrically and energetically. This provides a rationale of why the TS and the diradical intermediate are perturbed to nearly the same magnitude in energy, while the NPS principle causes the effect of radical stability to be relatively small.

The results suggest two general classes of reactants. For the “saturated molecules”, the energies of the transition states and intermediate radicals are influenced to almost the same extent. With “unsaturated molecules”, however, resonance stabilization is much less important in the transition state than in the product radical. Our observations are different from those observed by Shaik for H-abstraction by the Cytochrome P450 CpdI, where a linear relationship with a slope of 0.59 ($R^2 = 0.90$) between the barrier height and BDE is found,⁵¹ and propene and toluene fit on the same correlation as saturated substrates.^{37,51}

This difference in the formation of more or less localized radicals or those stabilized by hyperconjugation (“saturated” systems) and those stabilized by conjugation (“unsaturated”) is consistent with the “Principle of Non-Perfect Synchronization (NPS)”, which was proposed by Bernasconi.^{58–60} This principle was applied mainly to deprotonation reactions and carbanion stability, where delocalization is not very influential in stabilizing transition states.⁵⁸ There have been several observations by Tedder and Walton that the transition states of homolysis reactions are often imbalanced (bond cleavage and delocalization have unequal progress), and in particular that resonance stabilization in the product of a radical addition reaction develops ‘late’ on the reaction coordinate.^{61–63} In this case, the lag in the development of resonance stabilization of the transition state causes the barrier to be higher than expected on the basis of product stability. This results in a smaller slope for the barrier versus BDE plot. The lag can be indirectly tracked through the bond length of the breaking C–H bond and the C–C bond connecting the breaking C–H bond to the π bond. This length is a reflection of the strength of CH– π hyperconjugation. This C–C bond denoted with a red line in Table 2 was used as the measure of developing resonance stabilization. As shown here, the bond length of this C–C in the intermediate is much smaller than that in the transition state for all members of the “unsaturated group”. This is an indicator of a much stronger resonance stabilization in the product radical than in the transition state.

The nature of the transition state was explored by analyzing the charges and spins of two representative transition structures by NBO analysis in Figure 5, as inspired by the pioneering work by Shaik.^{64–66} The saturated compound (2) and the unsaturated (13) have a late and early transition state, respectively. Figure 5 illustrates that both transition states involve an almost charge neutral H-abstracted moiety with radical character. This indicates that these TSs have dominant hydrogen atom transfer (HAT) characters, albeit with some proton-coupled electron transfer (PCET) character, which is indicated by the Q_{CT} quantities that show charge transfer from substrate to the oxidant. Shaik also reported the occurrence of proton-coupled electron transfer (PCET) for activation of N–H and O–H by nonheme iron-oxo complexes.⁶⁶

Polar Effects. Oxidations of primary, secondary, and tertiary C–H bonds all fit on the same line for the “saturated group” and “unsaturated group” (see both Figure 3 and Table S1), indicating that steric and polar effects influence the transition state only to the similar extent that they change BDE. It should be noted that polar effects have been proposed by Tedder to

Table 2. C–C Bond Distances in the Reactants (R), Transition States (TS), Intermediate Radicals (R•)^a

compounds	r_{C-C} (RH)	r_{C-C} (TS)	r_{C-C} (R•)	
13		1.50	1.47	1.39
14		1.50	1.47	1.39
15		1.51	1.49	1.40
16		1.51	1.47	1.41
17		1.51	1.49	1.42
18		1.52	1.50	1.43
19		1.51	1.47	1.40
20		1.52	1.49	1.44
21		1.52	1.49	1.44
22		1.53	1.50	1.44
23		1.51	1.49	1.45
24		1.46	1.43	1.38
25		1.47	1.44	1.39
26		1.47	1.45	1.39

^aDistance values are given in Å.

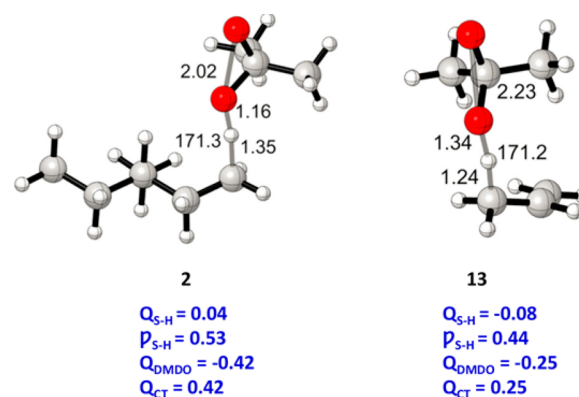


Figure 5. Geometric parameters (bond length in Å and angle in deg) along with NBO charges (Q) and spin densities (P) on the H-abstracted moiety (S–H), the charge on the oxidant (Q_{DMDO}), and the amount of charge transferred (Q_{CT}) from substrate to the oxidant in TS.

cause a deviation from the Evans–Polanyi correlation in the study of hydrogen abstraction by CH_3 and CF_3 radicals.^{36,62} In our work, a significant deviation by polar groups from the correlation is not observed, presumably because the current study does not involve functional groups with strong polarity. On the other hand, polar effects indeed generate some outliers

on the trend plot shown in Figure 3. As exemplified in Table 3, compounds 9 and 10 possess secondary C–H bonds with

Table 3. C–H Oxidation of Two Secondary C–H Bonds β or γ to the Inductively Electron-Withdrawing Acetate^a

C–H bond	ΔE_1^\ddagger	ΔH_1^\ddagger	$\Delta E_{\text{inter}}^\ddagger$	ΔE_d^\ddagger	ΔH_{rxn}	BDE
9	22.4	18.3	-2.6	25.1	7.1	96.3
10	23.0	19.0	-12.7	35.6	5.9	95.1

^aEnergies are given in kcal/mol.

different separations from the acetate group. Since it is close to the acetate, the CH bond in 9 involves a larger BDE (or ΔH_{rxn}). Curiously it has a lower activation barrier. This observation coincides with what Bach reported that polar effects may lower the reaction barrier by rendering an early transition state,⁶⁷ but simultaneously increase the BDE. In the current study, despite small deviations from the correlation plot, polar effects do not significantly affect the general trend. That is, polar effects both destabilize the radicals by reducing hyperconjugation and have a proportional effect on the activation barriers.

Distortion/Interaction Analysis. We explored the origins of reactivities and selectivities in the H-abstraction process of different substrates using the Distortion/Interaction model (see Table S1 and Figure 5). The substrates naturally divide into two groups of $\Delta E_{\text{inter}}^\ddagger$ values. Substrates 13–26 (“unsaturated group”) have much weaker interaction energies compared to other substrates 1–8 and 10–12; see Figure 6. Compound 9 is anomalous here, perhaps due to the polar effect. The interaction energies within each of these groups are very similar, varying only by 2 kcal/mol. There are remarkable linear

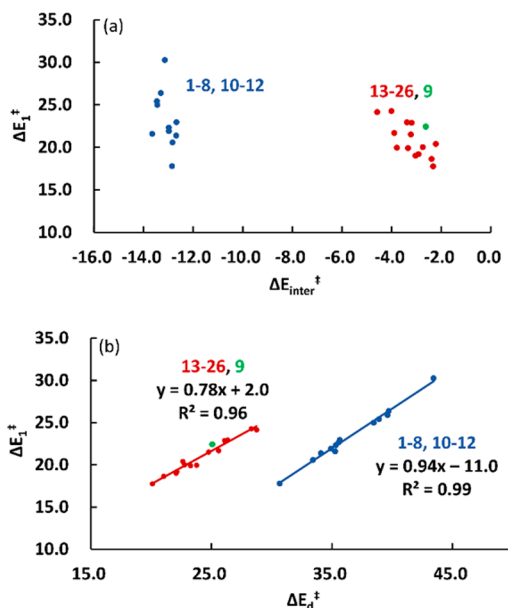


Figure 6. Plot of activation energy (ΔE_1^\ddagger) versus (a) interaction energy ($\Delta E_{\text{inter}}^\ddagger$) and (b) the total distortion energy (ΔE_d^\ddagger). Red dots are the substrates in the “unsaturated group”, the green dot is substrate 9, and blue dots are “saturated” substrates. Energies are given in kcal/mol.

correlations between activation energy and distortion energy for each group, with the correlation coefficients of 0.96 and 0.99, respectively.

Figure 7 shows plots of activation energies versus the bond lengths of the breaking C–H in the transition state, or the

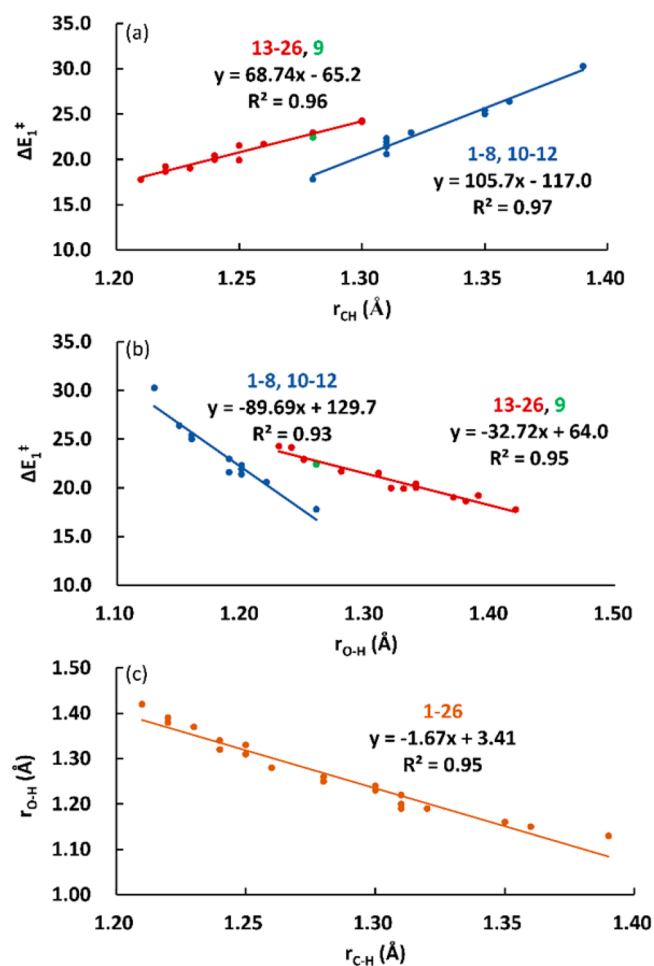


Figure 7. (a) Plot of activation energy (ΔE_1^\ddagger) versus C–H bond length ($r_{\text{C-H}}$) and (b) ΔE_1^\ddagger versus O–H bond length ($r_{\text{O-H}}$). Red dots are the substrates in the “unsaturated group”, the green dot is substrate 9, and blue dots are “saturated” substrates. (c) $r_{\text{O-H}}$ versus $r_{\text{C-H}}$. Orange points are all the substrates. Energies are given in kcal/mol.

forming O–H bond in the transition state. The two plotted bond lengths were also plotted versus each other and correlate closely. The substrates are again divided into the same way as before. The activation energy is decided by the degree of dissociation of the C–H bond or the formation of the O–H bond. The resonance effect in substrates 13–26 influences the degree of dissociation of the C–H bond, resulting in a much earlier transition state (obvious shortening of C–H bond and increasing of the O–H bond in the transition state); see Figure S1.

In order to understand the effect of early versus late transition state on the distortion and interaction energies, we performed a Distortion/Interaction analysis along the reaction coordinate. Substrates 2 and 4 were chosen as representatives for the “saturated group” and 13 for the “unsaturated group”. The activation energy for reaction of tertiary 4 (20.6 kcal/mol) is almost equal to the activation energy of allylic 13 (20.4 kcal/mol)

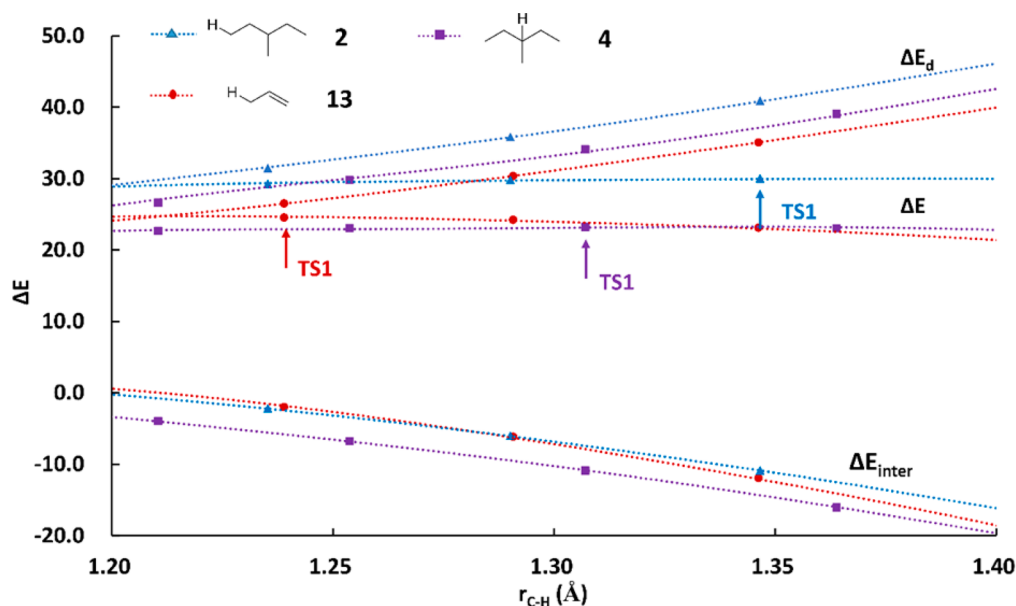


Figure 8. Distortion/Interaction analysis along the IRC (plotted as the C–H bond length). The energies by UB3LYP/6-31G(d) are given in kcal/mol.

mol). Figure 8 shows the energies along the IRC for the dioxirane reaction. The total energy, distortion energy, and interaction energy for each point along the reaction path were computed. The distortion energies follow the order of BDEs (84.0 kcal/mol for 13, 92.7 kcal/mol for 4, 98.0 kcal/mol for 2). At distances from 1.2–1.4 Å, there is a relatively small difference between the ΔE_d for 4 and 13 (~ 2.0 kcal/mol) compared to $\Delta\Delta BDE$ (~ 9.0 kcal/mol), while the $\Delta\Delta E_d$ (~ 3.5 kcal/mol) for 2 and 4 is more similar to $\Delta\Delta BDE$ (~ 5 kcal/mol). This is related to the observed NPS in that the difference in radical stability is not fully felt in the transition state. The interaction energies, arising from the $\sigma_{C-H}-\sigma_{O-O}^*$ interaction, are more stabilizing for the tertiary case, 4. The σ_{C-H} of 4 is at a higher energy than σ_{C-H} of 2, which enhances this interaction with the dioxirane σ_{O-O}^* orbital.

It is the lower distortion energy of the allylic or benzylic C–H bond that causes the transition state to be early. The transition state occurs where the increase in favorable ΔE_{inter} overcomes the increase in unfavorable ΔE_d . Most importantly, the high stabilization of the allylic or other unsaturated radicals is not manifested in the H-abstraction transition state. This is the origin of the NPS. All of these results show that the high reactivities of the members of the “unsaturated group” come from the lower distortion energy resulting from the conjugation effect, which shifts the transition state much earlier along the reaction coordinate and results in weaker interaction energies at the transition state. The Distortion/Interaction analysis along the C–H bond distance was also performed with calculations by the U ω B97X-D method, as shown in Figure S2. The same tendencies described above were found.

CONCLUSIONS

We have studied the origins of the reactivities and selectivities in DMDO C–H oxidations. We observed that separate linear relationships between activation energy and BDE occur for the “saturated” and “unsaturated” families of sp^3 C–H. The stabilities of the transition states are influenced much less than the stabilities of radicals for the “unsaturated group”. Resonance stabilization is much less important in the transition

state as compared to the product radical, because the transition states are “early”. The lower distortion energies of the “unsaturated” members for a given CH stretch are the origin of this effect. This effect is likely to be observed in all reactions involving CH breaking, but it has not been reported previously for other plots of ΔH^\ddagger versus ΔH_{rxn} or BDE perhaps because insufficient examples were studied to reveal this bimodal relationship. We are exploring this effect for other C–H activation reactions.

ASSOCIATED CONTENT

Supporting Information

The Supporting Information is available free of charge on the ACS Publications website at DOI: 10.1021/jacs.7b07988.

Benchmark for various DFT methods against CASPT2 and experiment, activation energies, distortion energies, BDE et al. for all the substrates, transition structures for all the substrates, Distortion/Interaction analysis with U ω B97X-D, Cartesian coordinates, charge, spin and energies (PDF)

AUTHOR INFORMATION

Corresponding Authors

*ymeimei@phy.ecnu.edu.cn

*houk@chem.ucla.edu

ORCID

Ye Mei: 0000-0002-3953-8508

K. N. Houk: 0000-0002-8387-5261

Notes

The authors declare no competing financial interest.

ACKNOWLEDGMENTS

We are grateful to the National Science Foundation (NSF) (CHE-1361104 and CHE-1464690), and the NSF under the CCI Center for Selective C–H Functionalization (CHE-1205646), the National Natural Science Foundation of China (Grant No. 21173082), and China Scholarship Council (CSC)

for financial support of this research. Calculations were performed on the Hoffman2 cluster at UCLA, the Extreme Science and Engineering Discovery Environment (XSEDE), which is supported by the NSF (OCI-1053575), and the Supercomputer Center at East China Normal University.

REFERENCES

- (1) Yamaguchi, J.; Yamaguchi, A. D.; Itami, K. *Angew. Chem., Int. Ed.* **2012**, *51*, 8960.
- (2) Doyle, M. P.; Goldberg, K. I. *Acc. Chem. Res.* **2012**, *45*, 777.
- (3) Crabtree, R. H. *Chem. Rev.* **2010**, *110*, 575.
- (4) de Montellano, P. R. O.; De Voss, J. J. *Nat. Prod. Rep.* **2002**, *19*, 477.
- (5) Groves, J. T. *Proc. Natl. Acad. Sci. U. S. A.* **2003**, *100*, 3569.
- (6) Qiu, Y. Y.; Gao, S. H. *Nat. Prod. Rep.* **2016**, *33*, 562.
- (7) Activation C–H. In *Topics in Current Chemistry*; Yu, J. Q., Shi, Z., Eds.; Springer: Berlin, 2010; Vol. 292.
- (8) Davies, H. M. L.; Beckwith, R. E. J. *Chem. Rev.* **2003**, *103*, 2861.
- (9) Mkhaliid, I. A. I.; Barnard, J. H.; Marder, T. B.; Murphy, J. M.; Hartwig, J. F. *Chem. Rev.* **2010**, *110*, 890.
- (10) Murray, R. W.; Jeyaraman, R. *J. Org. Chem.* **1985**, *50*, 2847.
- (11) Murray, R. W.; Jeyaraman, R.; Mohan, L. *J. Am. Chem. Soc.* **1986**, *108*, 2470.
- (12) Adam, W.; Curci, R.; Edwards, J. O. *Acc. Chem. Res.* **1989**, *22*, 205.
- (13) Curci, R.; Dinoi, A.; Rubino, M. F. *Pure Appl. Chem.* **1995**, *67*, 811.
- (14) Yang, Z.; Yu, P.; Houk, K. N. *J. Am. Chem. Soc.* **2016**, *138*, 4237.
- (15) Curci, R.; D'Accolti, L.; Fusco, C. *Acc. Chem. Res.* **2006**, *39*, 1.
- (16) Wender, P. A.; Hilinski, M. K.; Mayweg, A. V. W. *Org. Lett.* **2005**, *7*, 79.
- (17) Bruckl, T.; Baxter, R. D.; Ishihara, Y.; Baran, P. S. *Acc. Chem. Res.* **2012**, *45*, 826.
- (18) Chen, K.; Baran, P. S. *Nature* **2009**, *459*, 824.
- (19) Chen, K.; Richter, J. M.; Baran, P. S. *J. Am. Chem. Soc.* **2008**, *130*, 7247.
- (20) Newhouse, T.; Baran, P. S. *Angew. Chem., Int. Ed.* **2011**, *50*, 3362.
- (21) Lee, S.; Jamieson, D.; Fuchs, P. L. *Org. Lett.* **2009**, *11*, 5.
- (22) Mizuki, K.; Iwahashi, K.; Murata, N.; Ikeda, M.; Nakai, Y.; Yoneyama, H.; Harusawa, S.; Usami, Y. *Org. Lett.* **2014**, *16*, 3760.
- (23) Sikervar, V.; Fleet, J. C.; Fuchs, P. L. *J. Org. Chem.* **2012**, *77*, 5132.
- (24) Liu, W. L.; Li, X. K.; Chen, J.; Li, T. M.; Dong, M. Q.; Lei, X. G. *Chem. - Eur. J.* **2015**, *21*, 5345.
- (25) Fung, Y. S.; Yan, S. C.; Wong, M. K. *Org. Biomol. Chem.* **2012**, *10*, 3122.
- (26) Annese, C.; D'Accolti, L.; De Zotti, M.; Fusco, C.; Toniolo, C.; Williard, P. G.; Curci, R. *J. Org. Chem.* **2010**, *75*, 4812.
- (27) Annese, C.; Fanizza, I.; Calvano, C. D.; D'Accolti, L.; Fusco, C.; Curci, R.; Williard, P. G. *Org. Lett.* **2011**, *13*, 5096.
- (28) Annese, C.; D'Accolti, L.; Fusco, C.; Gandolfi, R.; Eaton, P. E.; Curci, R. *Org. Lett.* **2009**, *11*, 3574.
- (29) Annese, C.; D'Accolti, L.; Fusco, C.; Curci, R. *Org. Lett.* **2011**, *13*, 2142.
- (30) Chen, K.; Eschenmoser, A.; Baran, P. S. *Angew. Chem., Int. Ed.* **2009**, *48*, 9705.
- (31) Zou, L.; Paton, R. S.; Eschenmoser, A.; Newhouse, T. R.; Baran, P. S.; Houk, K. N. *J. Org. Chem.* **2013**, *78*, 4037.
- (32) González-Núñez, M. E.; Castellano, G.; Andreu, C.; Royo, J.; Báguena, M.; Mello, R.; Asensio, G. *J. Am. Chem. Soc.* **2001**, *123*, 7487.
- (33) González-Núñez, M. E.; Royo, J.; Mello, R.; Báguena, M.; Ferrer, J. M.; Ramírez de Arellano, C.; Asensio, G.; Prakash, G. K. S. *J. Org. Chem.* **2005**, *70*, 7919.
- (34) Chen, M. S.; White, M. C. *Science* **2010**, *327*, 566.
- (35) Chen, M. S.; White, M. C. *Science* **2007**, *318*, 783.
- (36) Tedder, J. M. *Angew. Chem., Int. Ed. Engl.* **1982**, *21*, 401.
- (37) Mayer, J. M. *Acc. Chem. Res.* **1998**, *31*, 441.
- (38) Shaik, S.; Shurki, A. *Angew. Chem., Int. Ed.* **1999**, *38*, 586.
- (39) Frisch, M. J.; Trucks, G. W.; Schlegel, H. B.; Scuseria, G. E.; Robb, M. A.; Cheeseman, J. R.; Scalmani, G.; Barone, V.; Mennucci, B.; Petersson, G. A.; Nakatsuji, H.; Caricato, M.; Li, X.; Hratchian, H. P.; Izmaylov, A. F.; Bloino, J.; Zheng, G.; Sonnenberg, J. L.; Hada, M.; Ehara, M.; Toyota, K.; Fukuda, R.; Hasegawa, J.; Ishida, M.; Nakajima, T.; Honda, Y.; Kitao, O.; Nakai, H.; Vreven, T.; Montgomery, J. A., Jr.; Peralta, J. E.; Ogliaro, F.; Bearpark, M.; Heyd, J. J.; Brothers, E.; Kudin, K. N.; Staroverov, V. N.; Keith, T.; Kobayashi, R.; Normand, J.; Raghavachari, K.; Rendell, A.; Burant, J. C.; Iyengar, S. S.; Tomasi, J.; Cossi, M.; Rega, N.; Millam, J. M.; Klene, M.; Knox, J. E.; Cross, J. B.; Bakken, V.; Adamo, C.; Jaramillo, J.; Gomperts, R.; Stratmann, R. E.; Yazyev, O.; Austin, A. J.; Cammi, R.; Pomelli, C.; Ochterski, J. W.; Martin, R. L.; Morokuma, K.; Zakrzewski, V. G.; Voth, G. A.; Salvador, P.; Dannenberg, J. J.; Dapprich, S.; Daniels, A. D.; Farkas, Ö.; Foresman, J. B.; Ortiz, J. V.; Cioslowski, J.; Fox, D. J. *Gaussian 09*, revision D.01; Gaussian, Inc.: Wallingford, CT, 2013.
- (40) Cremer, D.; Kraka, E.; Szalay, P. G. *Chem. Phys. Lett.* **1998**, *292*, 97.
- (41) Bach, R. D. *J. Phys. Chem. A* **2016**, *120*, 840.
- (42) Chai, J. D.; Head-Gordon, M. *Phys. Chem. Chem. Phys.* **2008**, *10*, 6615.
- (43) Shustov, G. V.; Rauk, A. *J. Org. Chem.* **1998**, *63*, 5413.
- (44) Bach, R. D.; Andres, J. L.; Su, M. D.; McDouall, J. J. W. *J. Am. Chem. Soc.* **1993**, *115*, 5768.
- (45) Bach, R. D.; Su, M.-D. *J. Am. Chem. Soc.* **1994**, *116*, 10103.
- (46) Fokin, A. A.; Tkachenko, B. A.; Korshunov, O. I.; Gunchenko, P. A.; Schreiner, P. R. *J. Am. Chem. Soc.* **2001**, *123*, 11248.
- (47) Freccero, M.; Gandolfi, R.; Sarzi-Amadè, M.; Rastelli, A. *J. Org. Chem.* **2003**, *68*, 811.
- (48) Park, J.-Y.; Harris, D. J. *Med. Chem.* **2003**, *46*, 1645.
- (49) Korzekwa, K. R.; Jones, J. P.; Gillette, J. R. *J. Am. Chem. Soc.* **1990**, *112*, 7042.
- (50) Kaizer, J.; Klinker, E. J.; Oh, N. Y.; Rohde, J.-U.; Song, W. J.; Stubna, A.; Kim, J.; Münck, E.; Nam, W.; Que, L. *J. Am. Chem. Soc.* **2004**, *126*, 472.
- (51) de Visser, S. P.; Kumar, D.; Cohen, S.; Shacham, R.; Shaik, S. *J. Am. Chem. Soc.* **2004**, *126*, 8362.
- (52) Ess, D. H.; Houk, K. N. *J. Am. Chem. Soc.* **2007**, *129*, 10646.
- (53) Hammond, G. S. *J. Am. Chem. Soc.* **1955**, *77*, 334.
- (54) Marcus, R. A. *J. Chem. Phys.* **1956**, *24*, 966.
- (55) Marcus, R. A. *J. Chem. Phys.* **1956**, *24*, 979.
- (56) Marcus, R. A.; Sutin, N. *Biochim. Biophys. Acta, Rev. Bioenerg.* **1985**, *811*, 265.
- (57) Brønsted, J. N.; Pedersen, K. J. *Zeitschrift für Phys. Chemie, Stöchiometrie und Verwandtschaftslehre* **1924**, *108*, 185.
- (58) Bernasconi, C. F. *Tetrahedron* **1985**, *41*, 3219.
- (59) Bernasconi, C. F. *Acc. Chem. Res.* **1987**, *20*, 301.
- (60) Bernasconi, C. F. *Acc. Chem. Res.* **1992**, *25*, 9.
- (61) Tedder, J. M.; Walton, J. C. In *Advances in Physical Organic Chemistry*; Gold, V., Bethell, D., Eds.; Academic Press: 1978; Vol. 16, p 51.
- (62) Tedder, J. M.; Walton, J. C. *Tetrahedron* **1980**, *36*, 701.
- (63) Walton, J. C. *J. Chem. Soc., Perkin Trans. 2* **1989**, *2*, 173.
- (64) Lai, W. Z.; Li, C. S.; Chen, H.; Shaik, S. *Angew. Chem., Int. Ed.* **2012**, *51*, 5556.
- (65) Li, C. S.; Danovich, D.; Shaik, S. *Chemical Science* **2012**, *3*, 1903.
- (66) Usharani, D.; Lacy, D. C.; Borovik, A. S.; Shaik, S. *J. Am. Chem. Soc.* **2013**, *135*, 17090.
- (67) Bach, R. D.; Thorpe, C.; Dmitrenko, O. *J. Phys. Chem. B* **2002**, *106*, 4325.